Research Article

For reprint orders, please contact: reprints@futuremedicine.com

Nanomedicine

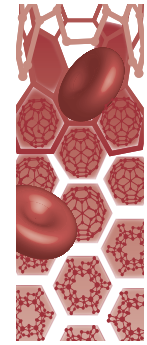

Inflammatory monocyte/macrophage modulation by liposome-entrapped spironolactone ameliorates acute lung injury in mice

Wen-Jie Ji[‡,1,2], Yong-Qiang Ma[‡,2], Xin Zhang[1], Li Zhang[3], Yi-Dan Zhang[1], Cheng-Cheng Su[1], Guo-An Xiang[1], Mei-Ping Zhang[3], Zhi-Chun Lin[1], Lu-Qing Wei[2], Peizhong P Wang[4], Zhuoli Zhang[1,5], Yu-Ming Li*[,1] & Xin Zhou**[,1]

[1]Tianjin Key Laboratory of Cardiovascular Remodeling & Target Organ Injury, Pingjin Hospital Heart Center, Tianjin 300162, China

[2]Department of Respiratory & Critical Care Medicine, Pingjin Hospital, Tianjin 300162, China

[3]Department of Pharmacognosy & Pharmaceutics, Logistics University of People's Armed Police Forces, Tianjin 300309, China

[4]Division of Community Health & Humanities, Faculty of Medicine, Memorial University of Newfoundland, Canada

[5]Department of Radiology, Northwestern University Feinberg School of Medicine, Chicago, IL 60611, USA

*Author for correspondence:
Tel.: +86 22 605 77282
cardiolab@live.com

**Author for correspondence:
Tel.: +86 22 605 78746
Fax: +86 22 846 19006
xzhou@live.com

‡Authors contributed equally

Aim: To examine the therapeutic/preventive potential of liposome-encapsulated spironolactone (SP; Lipo-SP) for acute lung injury (ALI) and fibrosis. **Materials & methods:** Lipo-SP was prepared by the film-ultrasonic method, and physicochemical and pharmacokinetic characterized for oral administration (10 and 20 mg/kg for SP-loaded liposome; 20 mg/kg for free SP) in a mouse model bleomycin-induced ALI. **Results:** Lipo-SP enhanced bioavailability of SP with significant amelioration in lung pathology. Mechanistically, SP-mediated mineralocorticoid receptor antagonism contributes to inflammatory monocyte/macrophage modulation via an inhibitory effect on Ly6C^{hi} monocytosis-directed M2 polarization of alveolar macrophages. Moreover, Lipo-SP at lower dose (10 mg/kg) exhibited more improvement in body weight gain. **Conclusion:** Our data highlight Lipo-SP as a promising approach with therapeutic/preventive potential for ALI and fibrosis.

First draft submitted: 5 January 2016; Accepted for publication: 11 April 2016; Published online: 12 May 2016

Keywords: acute lung injury • liposome • pulmonary fibrosis • spironolactone

Background

The past decade has witnessed an emerging role of monocyte/macrophage in a variety of inflammatory disease processes [1–3], which highlights a contribution of inflammatory monocyte/macrophage subsets mediated pro-inflammatory overactivation, tissue destruction, delayed resolution of inflammation and persistent fibrotic response, to organ fibrosis and failure [4–7]. Thus, modulating monocyte/macrophage phenotype switching, primarily, by inhibiting inflammatory subsets may serve as a treatment option for diseases dominated by overactivation of monocytes/macrophages [8–10].

Mineralocorticoid receptor (MR), as an intracellular receptor for aldosterone, its overactivation has been implicated as a key player in cardiovascular disease. Accordingly, pharmacological antagonism of MR using spironolactone (SP) is associated with improved cardiovascular outcomes [11,12]. To date, the beneficial role of MR antagonism has been mainly deemed to be achieved via a potassium-sparing-mediated diuretic and intrarenal effect. However, the recent discovery that mice lacking myeloid MR are protected against angiotension II-induced cardiac hypertrophy and fibrosis [13] opens a new avenue for extrarenal effects of aldosterone [14]. Recently, we and other group independently reported that systemic blockade of MR by SP could attenuate bleomycin (BLM)-induced acute lung injury (ALI) and fibrosis [15,16]; we also demonstrated an inhibitory effect of SP on MR-downstream signaling overactivation induced circulating Ly6C^{hi} monocytosis and alveolar macrophage M2 polarization [15].

Clinically, the benefit of SP is achieved only with long-term use via oral route, which is often associated with side effects of gynecomastia, menstrual irregularities and decreased libido due to its nonselective progesterone receptor agonistic and androgen receptor

Future Medicine part of fsg

antagonistic activity. Moreover, SP is characterized by incomplete oral behavior because of its low solubility (2.8 mg/100 ml at 25°C in water) and slow dissolution rate [17]. Liposome drug delivery systems have shown encouraging results in altering the bioavailability of encapsulated therapeutic agents, thus improving the drug therapeutic index in terms of longevity, targetability, drug safety profiles, therapeutic efficacy and distribution characteristics [18–20]. Additionally, liposomes can be engulfed by the mononuclear phagocyte system and is prone to recruit into the sites of inflammation due to increased vascular permeability via passive targeting [21]. Moreover, nanometric-sized drug delivery systems have been proposed to enhance the bioavailability of drug after oral administration [22]. Therefore, in the present study, we hypothesized that MR antagonism by SP-encapsulated liposomes via oral route can achieve enhanced SP bioavailability with therapeutic/preventive potential for ALI and lung fibrosis through modulating the inflammatory phenotypes of circulating monocytes/lung macrophages.

Materials & methods

Following guidelines from the Tianjin Municipal Science and Technology Commission (Regulations for Management of Experimental Animals, revised June 2004) and National Institutes of Health (publication no. 85-23, revised 1996), our study was approved by the Animal Use and Care Committee of Pingjin Hospital.

Materials

SP was obtained from Melonepharma Co., Ltd (Dalian, China). Soybean phosphatidylcholine was manufactured by Tywei Pharmaceutical Co., Ltd (Shanghai, China). Cholesterol was purchased from Aobox Biotechnology Co., Ltd (Beijing, China). BLM A5 was supplied from Taihe Pharmaceutical Co., Ltd (Tianjin, China). Antimouse CD11b-phycoerythrin (PE; clone M1/70), antimouse Ly6C-FITC (clone HK1.4), antimouse F4/80-PE-Cy5 (clone BM8), antimouse CD11c-PE-Cy7 (clone N418) and antimouse CD206-PE (clone C068C2) were all obtained from Biolegend, Inc. (CA, USA). TRIzol was purchased from Invitrogen (CA, USA). SYBR Green PCR Master Mix was obtained from Roche Diagnostics (IN, USA). A Tachypleus amebocyte lysate assay (China Horseshoe Crab Reagent Manufactory, Inc., Xiamen, China) was used to test for possible endotoxin contaminations of the liposomes. All other chemicals and solvents were of analytical grade.

Liposome preparation & characterization

In pilot studies, we have determined the optimal method for SP-encapsulated liposome (Lipo-SP) from three methods (film-ultrasonic [23], ethanol injection [24] and the reverse phase evaporation [25] methods) based on their encapsulation efficacy (EE%). The result showed that the film-ultrasonic method yielded the highest EE% (78.3%) when compared with the ethanol injection (77.5%) and the reverse phase evaporation (65.5%) methods. We next used orthogonal experimental design to optimize the prescription taking into account four factors (the ratio of drug to lipid, the ratio of cholesterol to lipid, the amount of Tween20 and the pH value of phosphate buffered saline (PBS) (Supplementary Tables 1 & 2). Specifically, soybean phosphatidylcholine, cholesterol and SP were dissolved in chloroform (weight ratio is 40:8:1) in a round-bottom flask. A lipid film was produced by a rotary evaporator and water bath with 50°C. The films were dried for 3 h to form dry lipid film under vacuum, and then resuspended in hydration buffer (PBS; pH 6.5) followed by vigorous stirring at room temperature for 1 h. The lipid suspensions were slightly sonicated with a sonicator at 200 W for 4 min over an ice bath. Then, we filtered the solution with a 0.22 μm filter and freeze-thawed it three-times with liquid nitrogen. Drug-loaded liposomes were stored at 2–8°C. Empty liposomes (Emp-Lipo) were prepared using the same protocol without SP.

The mean diameters, polydispersity and zeta potential of liposomes were measured using the dynamic light scattering instrument Zetasizer (Nano ZS, Malvern, UK). The morphology of the liposomes was characterized by a transmission electron microscope (JEOL, Japan). For liposome encapsulation assay, Lipo-SP suspension (3 ml) was first dialyzed against PBS (pH 7.4) using a dialysis bag for 6 h. The concentration of SP which was outside and inside of the dialysis bag was determined by high performance liquid chromatography (HPLC; LC-20AT, Shimadzu, Japan). Lipo-SP was dissolved in methanol, and 20 μl of the solution was injected into an octadecylsilane (ODS)-2 C18 columns (Hypersil ODS-2, 250 mm × 4.6 mm, 5 μm, Thermo Scientific, MA, USA) at 30°C. The mobile phase was consisted of methanol and water (70:30, V/V). The flow rate was 1.0 ml/min with detection at 238 nm. The EE% was calculated as follows:

$$EE\% = \frac{measured_{Drug} - unloaded_{Drug}}{measured_{Drug}}$$

For pharmacokinetic characterization of liposomes, 35 male C57BL/6 mice were orally administered via gavage with Lipo-SP or free spironolactone (Free-SP) (20 mg/kg SP). Blood samples were collected from the submandibular vein at 0, 0.5, 1.0, 2.0, 3.0, 4.0, 6.0, 12 and 24 h after administration. Plasma SP concentrations were analyzed by HPLC according to the above-

Table 1. Primer sequences used in this study.

Primers	Sequences (5′–3′)	PCR products (bp)
CCL2/MCP-1	TTAAGGCATCACAGTCCGAG	129
	TGAATGTGAAGTTGACCCGT	
TNF-α	TCTTCTCATTCCTGCTTGTGG	128
	GGTCTGGGCCATAGAACTGA	
IL-1β	AACGTGTGGGGGATGAATTG	130
	CATACTCATCAAAGCAATGT	
Arg-1	AGGAGAAGGCGTTTGCTTAG	115
	AGGAGAAGGCGTTTGCTTAG	
β-actin	CTAAGGCCAACCGTGAAAAG	104
	ACCAGAGGCATACAGGGACA	

mentioned methods. The pharmacokinetic parameters were calculated using the MultiFit program. For drug tissue biodistribution assays, 90 male C57BL/6 mice treated with BLM (see below; 1 h after oropharyngeal installation of BLM) were sacrificed by exsanguinations under ether anesthesia followed by a brief infusion of cold PBS via aorta at 0, 0.5, 1.0, 2.0, 3.0, 4.0, 6.0, 12 and 24 h after oral administration of Lipo-SP or Free-SP (20 mg/kg SP; n = 45 for each group). Their lungs, heart, kidneys, and liver were quickly harvested for SP concentration measurement. After weighing, tissue samples were rinsed with saline in the ratio 1:9 (W/V) by homogenization in a 4°C water bath and centrifuged at 20,000 × *g* for 10 min at 4°C. Then the drug concentration in supernatant was determined by HPLC.

Mouse model of ALI & fibrosis

Male C57BL/6 mice (Laboratory Animal Center of the Academy of Military Medical Sciences, Beijing, China) were lightly anesthetized by inhalation of ether, then BLM (2.5 mg/kg body weight in 40 µl saline) or saline (40 µl) was administered by oropharyngeal installation as described previously in our laboratory [15,26]. Animals were then randomly assigned into the following six groups: 0.9% saline (Saline) only; BLM only; BLM + empty liposomes (Emp-Lipo); BLM + Lipo-SP 10 mg/kg (Lipo-SP_10); BLM + Lipo-SP 20 mg/kg (Lipo-SP_20); and BLM + Free-SP 20 mg/kg (Free-SP_20). The doses for SP intervention were based on pharmacokinetic study and our previous work using free SP in BLM-challenged mice [15]. From the day of BLM installation (day 0), Emp-Lipo, Lipo-SP or Free-SP was delivered by oral gavage once daily, which was continued for 21 days. On days 1, 3, 7, 14 and 21, a total of 10–14 mice in each group were weighted and then euthanized by exsanguinations under ether anesthesia. Their blood, bronchoalveolar lavage fluid (BALF) and lung tissues were collected for further assays.

BALF & lung histology

BALF was collected with 1 ml of 0.9% sterile saline injected three times via right tracheal cannulation and centrifuged at 300 × *g* for 10 min at 4°C. The supernatant was collected for cytokine analyses. The remaining cell pellet was resuspended for cellular analyses, including total cell counts, differential cell counts and flow cytometry (FCM) analyses. Circulating monocytes and cells from BALF were subjected to FCM on a Cytomics FC500 cytometer (Beckman Coulter, FL, USA), which was analyzed using FlowJo software (Treestar, OR,

Table 2. Pharmacokinetic parameters of free spironolactone and liposome-entrapped spironolactone in mice (mean ± standard error of mean).

Parameters	Free-SP	Lipo-SP
C_{max} (ng/ml)	10.18 ± 2.43	23.13 ± 2.86†
T_{max} (h)	1.099 ± 0.301	1.089 ± 1.356
$t_{1/2}$ (h)	0.738 ± 0.188	0.736 ± 0.152
$AUC_{0-24\,h}$ (h ng/ml)	30.41 ± 2.87	68.44 ± 8.25†

†$p < 0.05$.
AUC_{0-24h}: Area under the plasma concentration-time curve; C_{max}: Maximum concentration; T_{max}: Time at which maximum concentration was observed; $t_{1/2}$: Apparent elimination half-life.

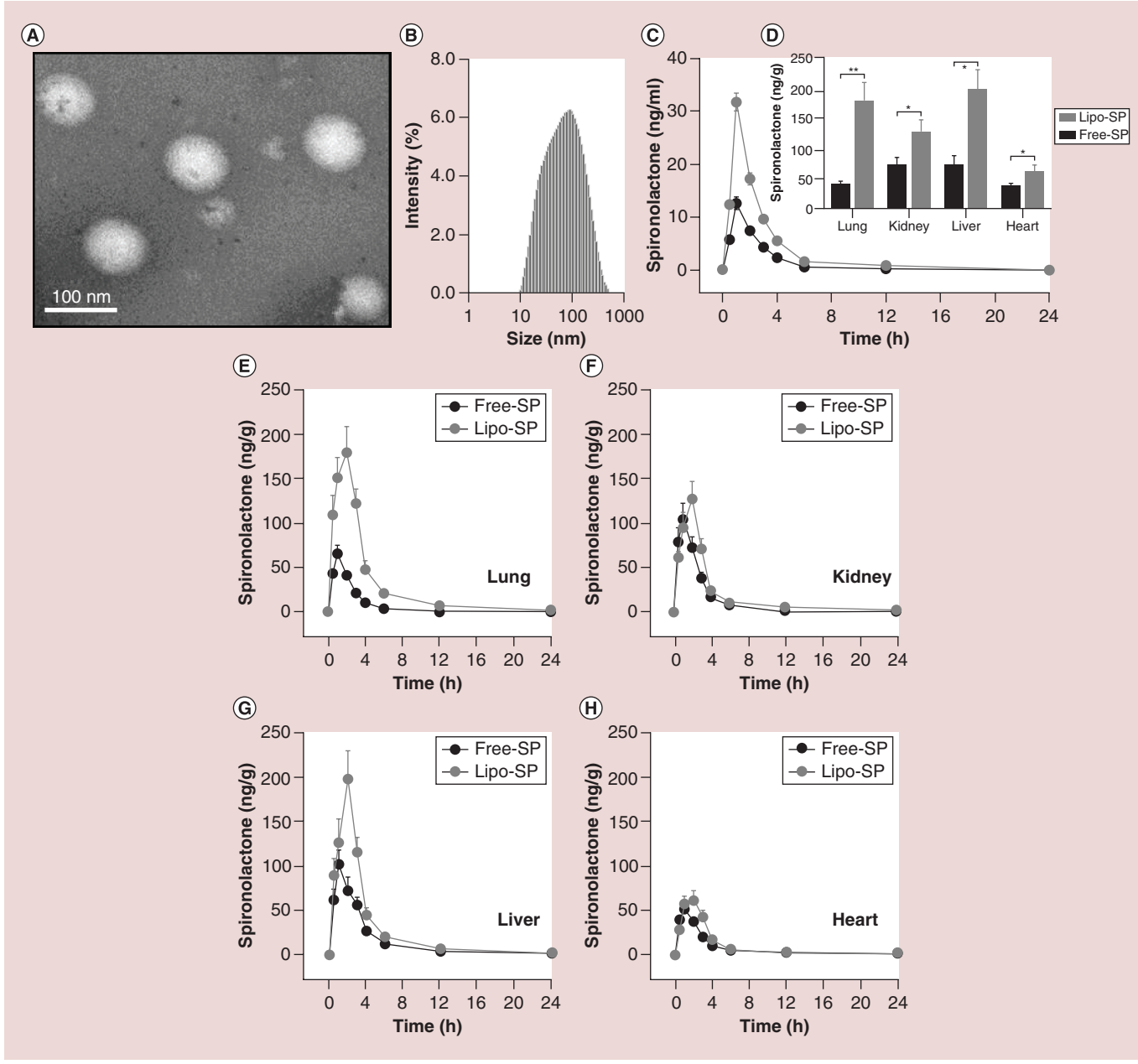

Figure 1. Liposome characterization: pharmacokinetics and biodistribution. **(A)** Representative transmission electrical microscopy of Lipo-SP; **(B)** diameter distribution of Lipo-SP; **(C)** plasma pharmacokinetic analysis of Lipo-SP and Free-SP in mice; **(D)** SP tissue distribution in bleomycin-treated mice 2 h following oral administration. *p < 0.05 (n = 5–7); and **(E–H)** dynamic profiles of SP organ distribution following oral administration.
Free-SP: Free spironolactone; Lipo-SP: Liposome-entrapped spironolactone; SP: Spironolactone.

USA). The gating strategies for analyzing circulating monocyte subsets and alveolar macrophages were according to our previous reports [15,26].

The left lung of each mouse (from which no BALF was harvested) was fixed in 4% paraformaldehyde solution at low pressure (10 mm H_2O) for 24 h. Paraffin-embedded sections were stained with hematoxylin-eosin (H.E.) or Masson's trichrome and examined on a light microscope (E600POL, Nikon, Tokyo, Japan). The severity of lung inflammation was quantified by a semiquantitative scoring method in a blinded fashion [27]. The extent of fibrosis was determined by using digital quantitative analysis (Image Pro Plus software version 4.5, Media Cybernetics, MD, USA).

The whole left lung collagen content was determined by the analysis of hydroxyproline level as pre-

viously described [28]. Absorbance was measured at 550 nm on a NanoDrop 2000c spectrophotometer (Thermo Scientific, MA, USA). Results were expressed as micrograms of per left lung.

Total RNA was isolated from bronchoalveolar lavage-derived cells and lung tissue using TRIzol reagent. Transcript levels were determined by SYBR Green PCR Master Mix, and performed on ABI Prism 7300 (Applied Biosystems, CA, USA) in triplicate. The primer sequences are shown in Table 1. To calculate the relative mRNA expression, the $2^{-\Delta\Delta Ct}$ method was used.

The levels of cytokines (including TNF-α), monocyte chemoattractant protein-1/chemokine (C–C motif) ligand 2 (CCL2), IL-1β and IL-4 in the BALF were measured by commercially available ELISA kits (R&D Systems, MN, USA), according to the manufacturer's instructions.

Statistical analysis

All data are presented as the mean ± standard error of mean. Statistical analysis was performed using GraphPad Prism 5.0 software (GraphPad, CA, USA). Statistical comparison of multiple groups was performed by one-way analysis of variance with the Bonferroni posthoc test. A two-tailed p-value of <0.05 was considered statistically significant.

Results

Physicochemical characterization of the liposomes

Transmission electron microscopic examination revealed that the Lipo-SP droplets were spherical in shape and no aggregation or fusion was observed (Figure 1A). The mean diameter and polydispersity index of Lipo-SP were 101.0 ± 2.0 nm (Figure 1B) and 0.379 ± 0.02, respectively, indicating that Lipo-SP was well distributed in the system, as well as maintaining drug stability during the manufacturing process. The zeta potential of Lipo-SP was -1.75 ± 0.05 mV. The optimized EE% and drug loading of Lipo-SP reached 85.3% ± 1.5% and 2.5% ± 0.2%, respectively. Moreover, the endotoxin content in all liposome batches used in the present work was below the detection limit (0.2 EU/mg) of a Tachypleus amebocyte lysate assay. Thus, the effect of bacterial components on the immune system could be excluded.

Pharmacokinetics & tissue distribution of Lipo-SP in mice

The blood concentration and time profiles for Lipo-SP and Free-SP after oral administration (both in a dose of 20 mg/kg) are shown in Figure 1C. Lipo-SP exhibited a significantly increased plasma concentrations at 0.5, 1, 2 and 3 h with a peak level on 1 h (all $p < 0.05$ vs Free-SP). The plasma pharmacokinetic parameters of Lipo-SP and Free-SP (C_{max}, T_{max}, $t_{1/2}$ and $AUC_{0-24\,h}$) are presented in Table 2. These results indicate that the liposomally entrapped SP had a more improved intestinal absorption and increased plasma concentration, as compared with Free-SP.

Then we examined tissue distribution of SP in BLM-treated mice (1 h after BLM challenge) following Lipo-SP and Free-SP oral administration (20 mg/kg). The dynamic profiling (Figure 1E–H) showed that Lipo-SP led to a significantly higher concentration in the lung and in the liver with peak level observed on 2 h following oral administration, whereas the peak levels of Free-SP occurred on 1 h after oral administration. Additionally, 2 h following oral administration, Lipo-SP significantly enhanced the tissue distribution of SP compared with Free-SP (Figure 1D). Because oral Lipo-SP with a dose of 20 mg/kg SP yielded a more than twofold increase of SP concentrations both in plasma and lung tissue than oral Free-SP with same dose, two doses, that is, 10 and 20 mg/kg SP, were then chosen for Lipo-SP intervention study compared Free-SP at a dose of 20 mg/kg.

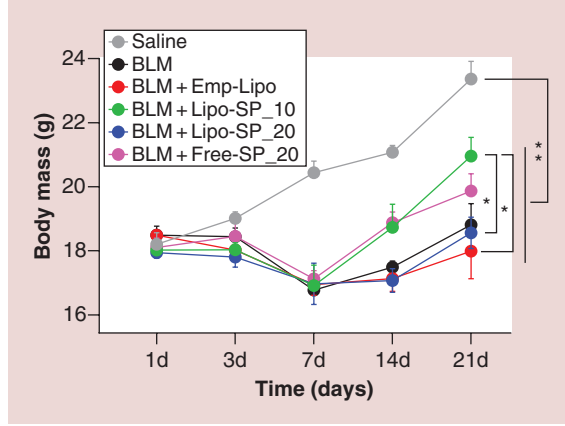

Figure 2. Dynamic changes in body weight following bleomycin challenge in mice. n = 5–7.
*p < 0.05; **p < 0.01.
BLM: Bleomycin; Emp-Lipo: Empty liposomes; Free-SP: Free spironolactone; Lipo-SP: Liposome-entrapped spironolactone.

Animal body weigh changes during intervention

As shown in Figure 2, there was a gradual gain in body weight in the Saline group. A dramatic drop in body weight of all BLM-challenged mice was observed on day 7, which then followed by a gradual increase, with significant improvement in Lipo-SP_10 and Free-SP_20 groups. On day 21, the mice in Lipo-SP_10 group exhibited an increased body weight compared with those in Emp-Lipo and Lipo-SP_20 groups.

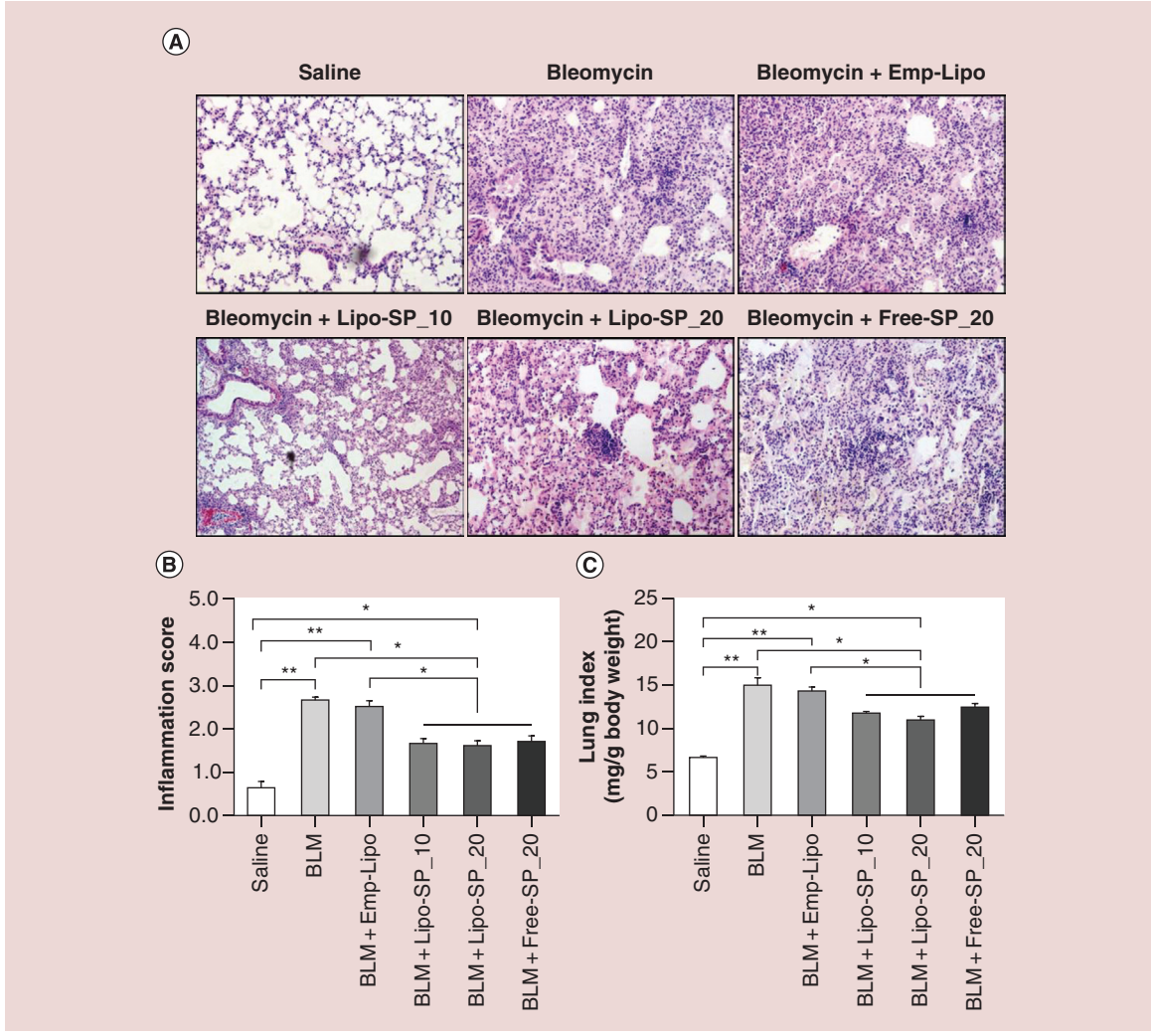

Figure 3. Hemotoxylin and eosin stained lung tissue and comparisons of the semi-quantitative inflammation scores and lung index on day 7 of bleomycin challenge. **(A)** Representative hemotoxylin and eosin staining images; **(B)** lung inflammation score comparisons; **(C)** lung index comparisons. n = 5–7.
*p < 0.05; **p < 0.01.
BLM: Bleomycin; Emp-Lipo: Empty liposomes; Free-SP: Free spironolactone; Lipo-SP: Liposome-entrapped spironolactone.

Effect of Lipo-SP on BLM-induced lung inflammation

Representative images of lung histology of acute phase inflammation (day 7) after BLM challenge (H.E. staining) are shown in Figure 3A. There was no apparent inflammatory response in the Saline group. An overt acute inflammatory response was noted in BLM and BLM+Emp-Lipo groups. SP interventions, both by Lipo-SP and Free-SP, significantly reduced pulmonary inflammation, as compared with BLM and BLM+Emp-Lipo groups (Figure 3B), whereas no obvious difference was observed between different SP formulations/doses. Similar improvement in lung index by SP interventions was also observed (Figure 3C). Additionally, differential cell counting in BALF on day 7 revealed that both Lipo-SP and Free-SP significantly reduced BLM-induced macrophage, lymphocyte and neutrophil infiltration in alveoli, whereas there was no significant difference between different formulations/doses (Figure 4).

The levels of inflammatory and profibrotic cytokines in BALF and related gene expression levels in lung tissue are shown in Figure 5. Compared with BLM and BLM+Emp-Lipo groups, CCL2 and IL-1β protein levels in BALF and mRNA levels in lung tissue were significantly downregulated in Lipo-SP and Free-SP groups both on day 3 and day 7. TNF-α mRNA level in lung tissue was downregulated in Lipo-SP and Free-SP groups (all $p < 0.05$). A trend for decreased TNF-α level in BALF was observed in Lipo-SP and Free-SP

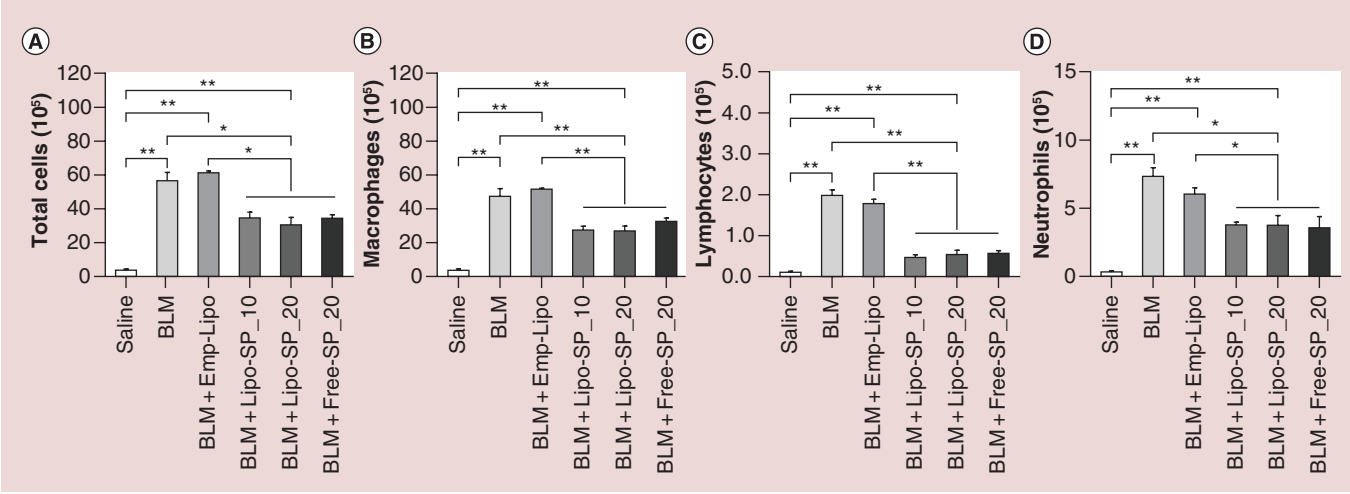

Figure 4. Differential cell counting from bronchoalveolar lavage fluid harvested on day 7. n = 5–7.
*p < 0.05; **p < 0.01.
BLM: Bleomycin; Emp-Lipo: Empty liposomes; Free-SP: Free spironolactone; Lipo-SP: Liposome-entrapped spironolactone.

groups on day 3 (nonsignificant decrease), and reached statistical significances on day 7, compared with BLM and BLM+Emp-Lipo groups.

Effect of Lipo-SP on BLM-induced lung fibrosis

On day 21 after BLM administration, compared with the Saline group, severe pulmonary fibrosis, as shown by Masson's trichrome staining and lung hydroxyproline content, was observed in the lungs from BLM and BLM+Emp-Lipo groups. SP interventions, both by Lipo-SP and Free-SP, significantly reduced BLM-induced lung fibrosis, compared with BLM and BLM+Emp-Lipo groups (all $p < 0.05$, Figure 6). There was a trend toward more fibrosis-reducing effect by Lipo-SP over Free-SP intervention, whereas no statistical significance was observed.

Effects of Lipo-SP on BLM-induced Ly6C^{hi} monocytosis & alveolar macrophage M2 polarization

Our previous work showed that there was a rapid expansion of circulating Ly6C^{hi} monocytes which peaked on day 3 of BLM challenge, as well as an expansion of M2-like alveolar macrophages with peak level on day 14 of BLM challenge, whose magnitudes are positively associated with disease severity [26]. In the present work, FCM analysis on day 3 revealed a significant reduction in circulating Ly6C^{hi} monocytes by Lipo-SP and Free-SP (Ly6C^{lo} subset presented with a reciprocal change), compared with BLM and BLM+Emp-Lipo groups (Figure 7A–C). Additionally, BLM-induced alveolar macrophage M2 polarization (F4/80+CD11c+CD206+) on day 14 was partially but significantly normalized by Lipo-SP and Free-SP toward M1 polarization (F4/80+CD11c+CD206-; see Figure 7D–F). There was a trend toward reductions in Ly6C^{hi} monocytes and M2 alveolar macrophages by Lipo-SP_20 compared with Lipo-SP_10, whereas no statistical significance was observed. Moreover, markers for M2 polarization, that is, IL-4 protein concentration in BALF (Figure 8A), Arg-1 mRNA level in lung tissue (Figure 8B) and in bronchoalveolar lavage cells (Figure 8C) on day 7 were also downregulated by Lipo-SP and Free-SP (all $p < 0.05$).

Discussion

In this study, to examine the therapeutic/preventive potentials of liposomally entrapped SP on a mouse model of ALI and fibrosis, we demonstrated that orally administered Lipo-SP could enhance the bioactivity of SP and contribute to an increased SP concentration in the lung with inflammatory injury (increased drug concentration liver as well); Lipo-SP with two doses (10 and 20 mg/kg) yielded similar improvements as compared with Free-SP in 20 mg/kg following oral administration, in terms of lung histology, cytokine expression profiles and inflammatory monocyte/macrophage modulation. Notably, lower dose of Lipo-SP (10 mg/kg) led to a more improvement in body weight following ALI. As we started SP intervention 1 h post-BLM exposure, at which time point lung edema and alveolitis could be induced [29], the interventional effect of SP on ALI and fibrosis could be regarded as therapeutic and preventive, respectively. Thus, our data suggest that SP administration by nanometric-sized drug delivery system via oral route is a novel therapeutic/preventive approach for ALI and fibrosis.

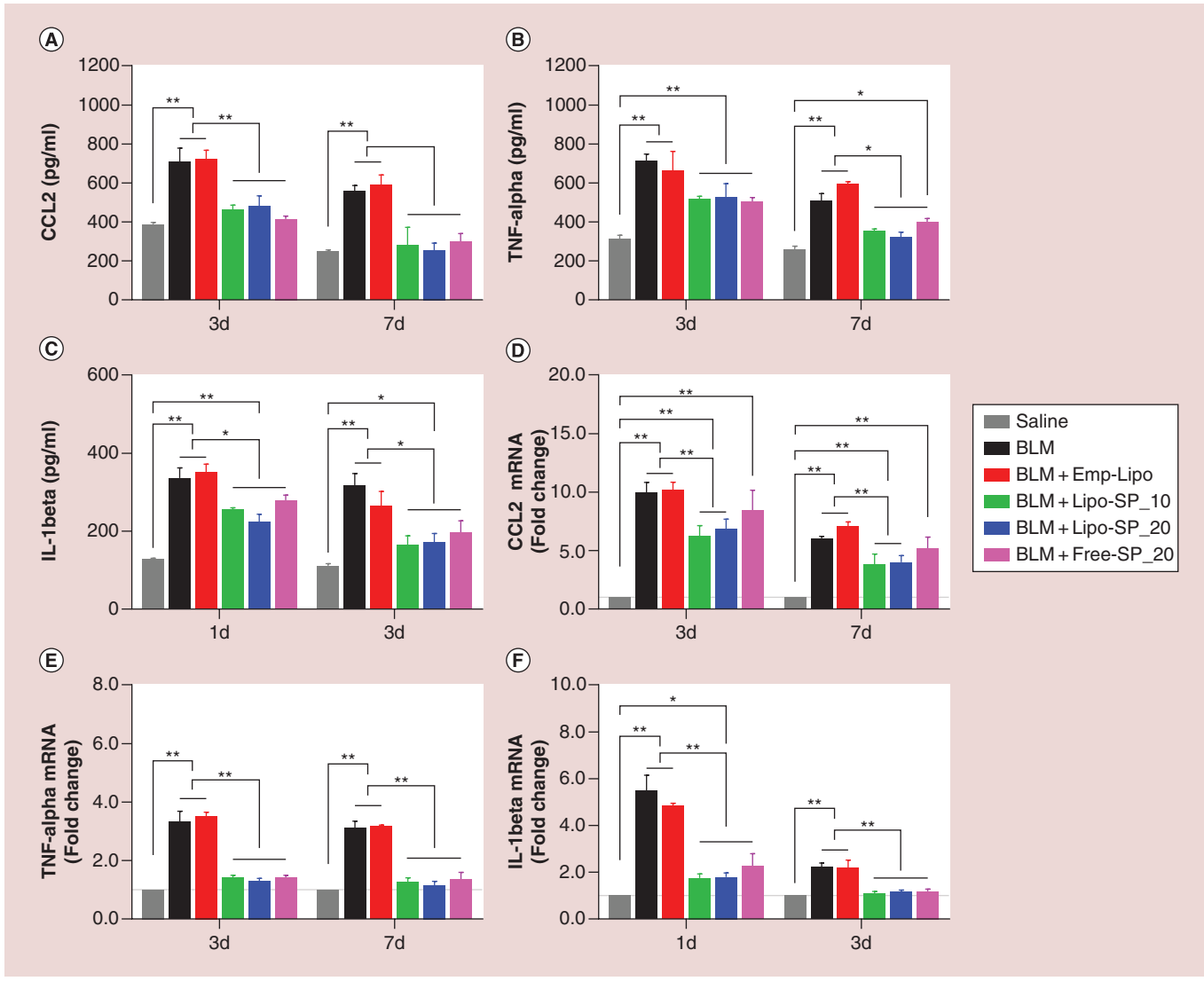

Figure 5. The protein levels of chemokine (C–C motif) ligand 2. TNF-α and IL-1β in bronchoalveolar lavage fluid detected by ELISA at selected time points **(A–C)** and the related mRNA levels in lung tissue **(D–F)**. n = 5–7.
*p < 0.05; **p < 0.01.
BLM: Bleomycin; Emp-Lipo: Empty liposomes; Free-SP: Free spironolactone; Lipo-SP: Liposome-entrapped spironolactone.

SP is a US FDA approved potassium-sparing diuretics with a long history of clinical use, and its unique role in clinical practice has been recently re-evaluated and emphasized for the treatment of resistant hypertension [30]. The antihypertensive and antifibrotic effect of SP requires long-term use, which makes intravenous approach less attractive. Therefore, in the present study, we only compared therapeutic/preventive effects of Lipo-SP with Free-SP via oral administration. Despite the fact that orally administered nanometric-sized drug delivery system could contribute to drug bioavailability enhancement, there are several critical considerations to evaluate the therapeutic efficacy, especially the gastrointestinal barrier that may impact nanocarrier's integrity and physicochemical features (particle size and surface composition), which ultimately influence the optimal transport of drug into the circulation [22]. For example, the exposure of nanocarriers to gastrointestinal environment, with alterations in pH, ionic strength, redox potential and enzymatic activities, may lead to instability and degradation of particles [22,31]. Admittedly, we cannot provide with direct evidence on the existence of intact Lipo-SP in bloodstream following oral administration. Thus, the enrichment of SP concentration in lung tissue with inflammatory injury could be explained as an indication for the passive targeting of Lipo-SP.

Notably, in the present work, the possible engulfment

of Lipo-SP by monocytes/macrophages is involved in Lipo-SP-mediated lung SP concentration enrichment, because orally administered Lipo-SP also contributes to an increased SP concentration in liver, suggesting potential uptake of liposomes by liver-residing macrophages, Kupffer cells. Emerging evidence showed that circulating monocytes and alveolar macrophages play important roles in ALI and fibrosis [26,32,33]. Precisely, ALI-induced circulating inflammatory Ly6C^{hi} monocyte mobilization from bone marrow and spleen [34] contributes to Ly6C^{hi} monocyte infiltration in lung tissue [35–38], which leads to a parallel increase of M2-like macrophages in alveolar compartment (either by direct differentiation or by paracrine effects). The severity and persistency of M2 polarization in alveolar macrophages would ultimately result in delayed resolution of inflammation and consequently, pulmonary fibrosis [36,39]. Thus, this Ly6C^{hi} monocyte-directed alveolar macrophage M2 polarization is a key pathophysiological process for ALI and fibrosis. Here, we have shown that in agreement with systemic SP use, Lipo-SP intervention contributes to a modulatory role between proinflammatory and anti-inflammatory monocyte/macrophage-mediated paracrine effect as well, which is shown by altered local cytokine expression profiles favoring a microenvironment to suppress pulmonary inflammation and fibrosis. The efficacy of MR antagonism by SP is also supported by the decreased levels of CCL2 and IL-1β after Lipo-SP and Free-SP intervention in this study, because the expression of these two cytokines, as the core components involved in inflammatory as well profibrotic response, is both dependent

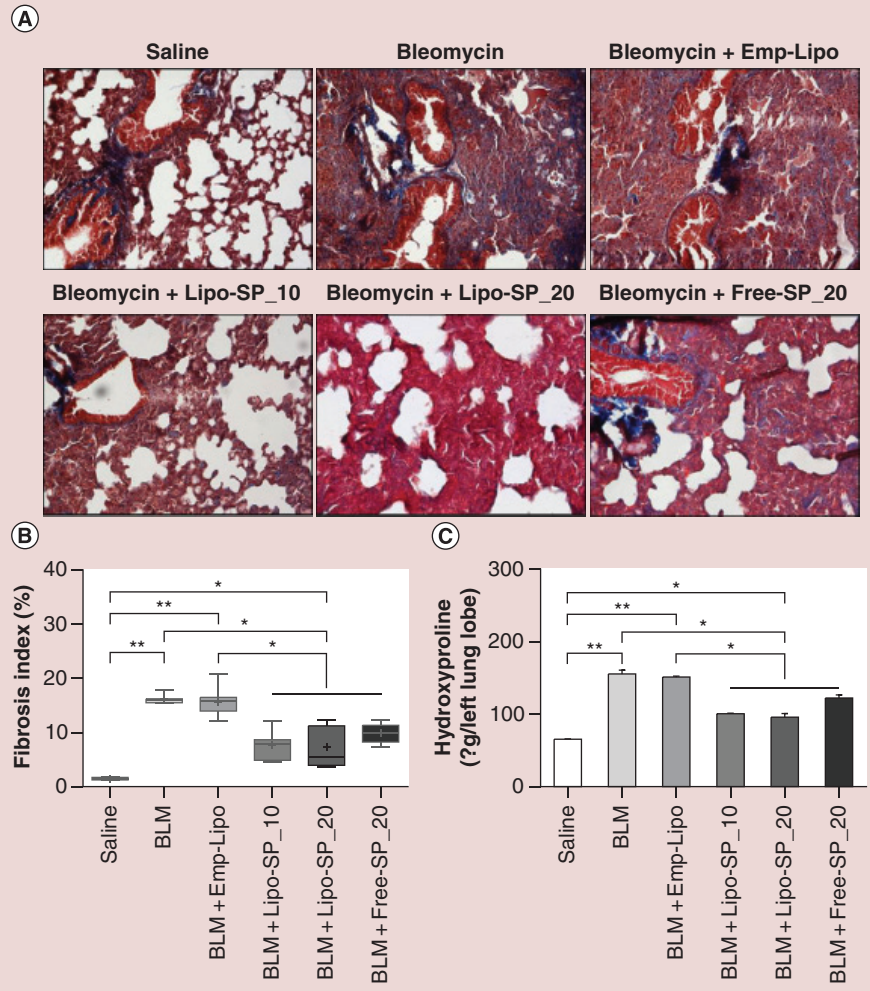

Figure 6. Masson's trichrome stained lung tissue: fibrosis index and total lung hydroxyproline content on day 21 after bleomycin challenge. **(A)** Representative Masson's trichrome staining images; **(B)** lung fibrosis index; **(C)** lung Hyp content. n = 5–7.
*p < 0.05; **p < 0.01.
BLM: Bleomycin; Emp-Lipo: Empty liposomes; Free-SP: Free spironolactone; Hyp: Hydroxyproline; Lipo-SP: Liposome-entrapped spironolactone.

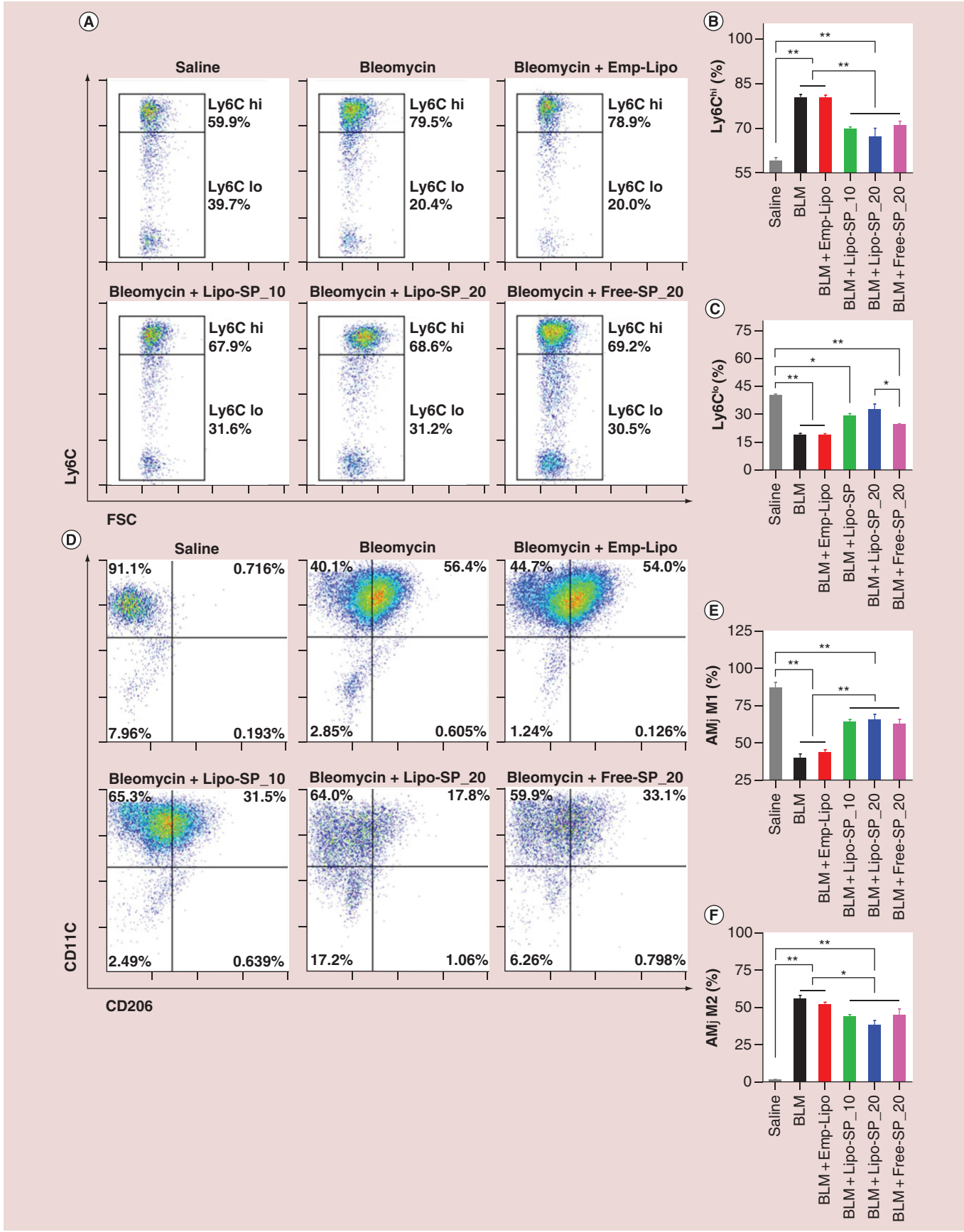
A
Saline
Ly6C hi 59.9%
Ly6C lo 39.7%
Bleomycin
Ly6C hi 79.5%
Ly6C lo 20.4%
Bleomycin + Emp-Lipo
Ly6C hi 78.9%
Ly6C lo 20.0%
Bleomycin + Lipo-SP_10
Ly6C hi 67.9%
Ly6C lo 31.6%
Bleomycin + Lipo-SP_20
Ly6C hi 68.6%
Ly6C lo 31.2%
Bleomycin + Free-SP_20
Ly6C hi 69.2%
Ly6C lo 30.5%
Ly6C
FSC
B
Ly6C^hi (%)
C
Ly6C^lo (%)
D
Saline
91.1% 0.716% 7.96% 0.193%
Bleomycin
40.1% 56.4% 2.85% 0.605%
Bleomycin + Emp-Lipo
44.7% 54.0% 1.24% 0.126%
Bleomycin + Lipo-SP_10
65.3% 31.5% 2.49% 0.639%
Bleomycin + Lipo-SP_20
64.0% 17.8% 17.2% 1.06%
Bleomycin + Free-SP_20
59.9% 33.1% 6.26% 0.798%
CD11C
CD206
E
AMj M1 (%)
F
AMj M2 (%)
Saline
BLM
BLM + Emp-Lipo
BLM + Lipo-SP_10
BLM + Lipo-SP_20
BLM + Free-SP_20

Figure 7. Flow cytometry analysis of circulating monocyte subsets (Ly6C^{hi} and Ly6C^{lo}) on day 3 (A–C) and alveolar macrophage M1 (F4/80+CD11c+CD206-) and M2 (F4/80+CD11c+CD206+) polarization (D–F) on day 14 of bleomycin challenge (see facing page). n = 5–7. *p < 0.05; **p < 0.01.
AMφ: Alveolar macrophages; BLM: Bleomycin; Emp-Lipo: Empty liposomes; Free-SP: Free spironolactone; FSC: Forward-scattered light; Lipo-SP: Liposome-entrapped spironolactone.

on MR-downstream signaling [40,41]. Therefore, our data support the emerging concept that active elimination and subsequent degradation of drug-loaded liposomes by monocytes/macrophages is a novel approach for the treatment of diseases dominated by monocyte/macrophage-mediated pathogenesis [42,43].

In this work, we did not find obvious difference between two doses of Lipo-SP in terms of lung pathology and monocyte/macrophage modulation, suggesting 10 mg/kg Lipo-SP as the plateau dose for SP's therapeutic window in our model. However, Lipo-SP with lower dose (10 mg/kg) is associated with a more improvement in body weight. There is accumulating evidence showing that the renin–angiotensin–aldosterone system (RAAS) is critically involved in fluid and energy balance regulation [44], and inhibition renin–angiotensin–aldosterone system is associated with reduce body weight [45,46]. Obviously, lower dose of Lipo-SP with enhanced bioavailability, would bring potential safety advantage during the rehabilitation period following ALI.

The present work is focusing on the liposome-mediated drug bioavailability enhancement via oral route. It should be noted that, to target inflammatory response following ALI, pulmonary endothelium targeting via intravenous route by liposome-mediated delivery of antisense oligodeoxyonucleotides [47] and liposome-encapsulated antioxidant molecule delivery [48] is a promising approach. Additionally, particular interest is also focused on the pulmonary route by aerosolization or inhalation of colloidal systems [49,50], which is characterized by a high surface area with rapid absorption due to high vascularization and circumvention of the first pass effect [51]. Thus, future work is warranted to examine the effect of Lipo-SP on ALI and fibrosis via pulmonary route.

Our study has the following limitations. First, as our work is focused on the therapeutic/preventive effect of SP with inflammatory monocyte/macrophage targeting, we did not use myeloid-specific MR knockout mice, which may be an ideal model to fully characterize the molecular pathways associated with therapeutic response to SP. Second, to dissect the contribution of monocyte/macrophage in ALI and fibrosis, a routinely used approach is clodronate-liposome-mediated mononuclear phagocyte depletion. However, this method could eliminate monocyte/macrophage without subpopulation selection, thus may not be suitable for pharmacological studies, and may also lead to complex results to interpret. Third, as the major purpose of the present study is to confirm liposome drug-carrier-mediated SP bioavailability enhancement via oral route, it is a technical challenge to provide direct evidence showing the existence of intact liposomes in peripheral circulation following oral administration. However, to address this issue, a promising effort is underway to integrate FCM and pharmacokinetic anal-

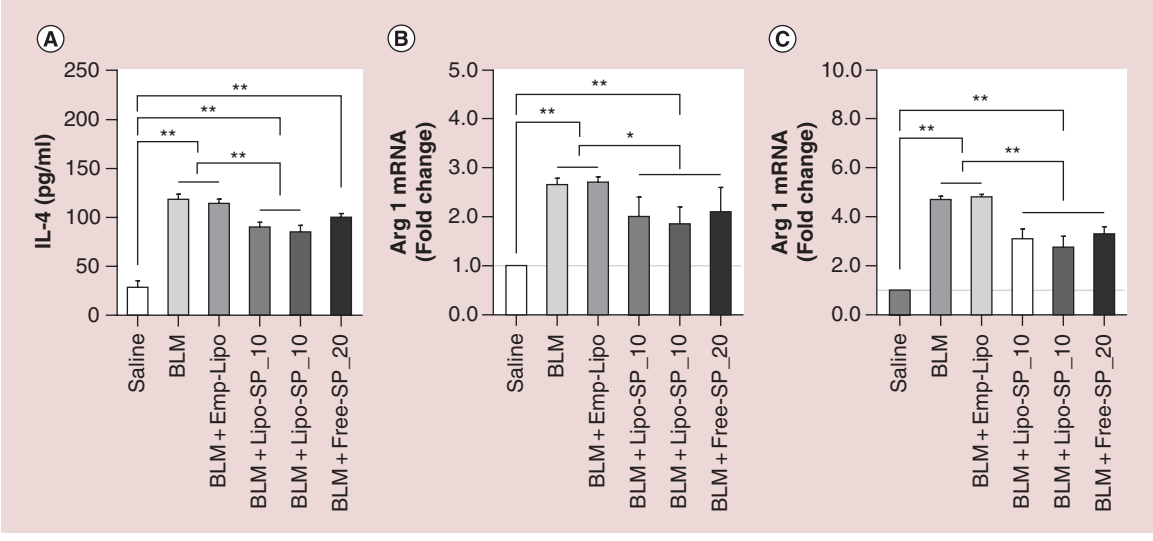

Figure 8. The protein level of IL-4 in bronchoalveolar lavage fluid detected by ELISA on day 7 (A) and the expression of arginase-1 mRNA in lung tissue (B) and in bronchoalveolar lavage cells (C) on day 7. n = 5–7. *p < 0.05; **p < 0.01.
BLM: Bleomycin; Emp-Lipo: Empty liposomes; Free-SP: Free spironolactone; Lipo-SP: Liposome-entrapped spironolactone.

yses using techniques described previously [52]. Forth, to better profile higher SP dose-associated side effects, such as gynecomastia, a full characterization of biochemical and pathological alterations in mammary glands is warranted in future work.

In summary, our work for the first time confirms the enhanced bioavailability of Lipo-SP via oral route with therapeutic/preventive potential in a mouse model of ALI and fibrosis; mechanistically, SP-mediated MR antagonism contributes to inflammatory monocyte/macrophage modulation, via an inhibitory effect on Ly6C^{hi} monocytosis-directed M2 polarization of alveolar macrophages. Our data highlight Lipo-SP as an effective and promising therapeutic/preventive approach for ALI and fibrosis.

Financial & competing interests disclosure

This work was supported by National Natural Science Foundation of China (81102088, 81170238, 81441101 and 81570335) and Tianjin Municipal Science and Technology Committee (12JCYBJC16600, 11JCYBJC11800, 13JCYBJC22000, 15ZXJZSY00010 and 15JCZDJC35000). The authors have no other relevant affiliations or financial involvement with any organization or entity with a financial interest in or financial conflict with the subject matter or materials discussed in the manuscript apart from those disclosed.

No writing assistance was utilized in the production of this manuscript.

Ethical conduct of research

The authors state that they have obtained appropriate institutional review board approval or have followed the principles outlined in the Declaration of Helsinki for all human or animal experimental investigations. In addition, for investigations involving human subjects, informed consent has been obtained from the participants involved.

Executive summary

Background

- Mineralocorticoid receptor (MR) antagonism exerts an inhibitory effect on inflammatory monocyte/macrophage activation and organ fibrosis after tissue injury.
- MR antagonism by spironolactone (SP)-encapsulated liposomes (Lipo-SP) via oral route may achieve enhanced SP bioavailability with therapeutic/preventive potential for acute lung injury (ALI) and lung fibrosis through modulating the inflammatory phenotypes of circulating monocytes/lung macrophages.

Materials & methods

- Lipo-SP was prepared using the film-ultrasonic method and physicochemically and pharmacokinetically characterized for oral administration in mice.
- Therapeutic/preventive potential of orally administered Lipo-SP (10 and 20 mg/kg) was compared with free spironolactone (20 mg/kg) in a mouse model of bleomycin-induced ALI.

Results & discussion

- Orally administered Lipo-SP could enhance the bioactivity of SP, and contribute to an increased SP concentration in the lung after bleomycin exposure.
- Lipo-SP with two doses yielded similar improvements in lung histology and cytokine expression profiles as compared with free spironolactone, whereas lower dose of Lipo-SP (10 mg/kg) was associated with more improvement in body weight following ALI.
- SP-mediated MR antagonism contributes to inflammatory monocyte/macrophage modulation via an inhibitory effect on Ly6C^{hi} monocytosis-directed M2 polarization of alveolar macrophages.

Conclusion & future perspective

- This is the first study confirming the enhanced bioavailability of Lipo-SP via oral route in a mouse model of ALI and fibrosis.
- Lipo-SP is a promising approach with therapeutic/preventive potential for ALI and fibrosis via a modulatory effect on phenotype switch of inflammatory monocytes/macrophages.

References

Papers of special note have been highlighted as: • of interest; •• of considerable interest

1 Chow A, Brown BD, Merad M. Studying the mononuclear phagocyte system in the molecular age. *Nat. Rev. Immunol.* 11(11), 788–798 (2011).

2 Scott CL, Henri S, Guilliams M. Mononuclear phagocytes of the intestine, the skin, and the lung. *Immunol. Rev.* 262(1), 9–24 (2014).

3 Swirski FK, Robbins CS, Nahrendorf M. Development and function of arterial and cardiac macrophages. *Trends Immunol.* 37(1), 32–40 (2016).

4 Haldar M, Murphy KM. Origin, development, and homeostasis of tissue-resident macrophages. *Immunol. Rev.* 262(1), 25–35 (2014).

5 Ginhoux F, Jung S. Monocytes and macrophages: developmental pathways and tissue homeostasis. *Nat. Rev. Immunol.* 14(6), 392–404 (2014).

6 Ismahil MA, Hamid T, Bansal SS, Patel B, Kingery JR, Prabhu SD. Remodeling of the mononuclear phagocyte network underlies chronic inflammation and disease progression in heart failure: critical importance of the cardiosplenic axis. *Circ. Res.* 114(2), 266–282 (2014).

7 Tacke F, Zimmermann HW. Macrophage heterogeneity in liver injury and fibrosis. *J. Hepatol.* 60(5), 1090–1096 (2014).

8 Leuschner F, Dutta P, Gorbatov R *et al*. Therapeutic siRNA silencing in inflammatory monocytes in mice. *Nat. Biotechnol.* 29(11), 1005–1010 (2011).

9 Harel-Adar T, Ben Mordechai T, Amsalem Y, Feinberg MS, Leor J, Cohen S. Modulation of cardiac macrophages by phosphatidylserine-presenting liposomes improves infarct repair. *Proc. Natl Acad. Sci. USA* 108(5), 1827–1832 (2011).

10 Zhou X, Luo YC, Ji WJ *et al*. Modulation of mononuclear phagocyte inflammatory response by liposome-encapsulated voltage gated sodium channel inhibitor ameliorates myocardial ischemia/reperfusion injury in rats. *PLoS One* 8(9), e74390 (2013).

11 Hamaguchi S, Kinugawa S, Tsuchihashi-Makaya M *et al*. Spironolactone use at discharge was associated with improved survival in hospitalized patients with systolic heart failure. *Am. Heart J.* 160(6), 1156–1162 (2010).

12 Song PS, Kim DK, Seo GW *et al*. Spironolactone lowers the rate of repeat revascularization in acute myocardial infarction patients treated with percutaneous coronary intervention. *Am. Heart J.* 168(3), 346–353 (2014).

13 Usher MG, Duan SZ, Ivaschenko CY *et al*. Myeloid mineralocorticoid receptor controls macrophage polarization and cardiovascular hypertrophy and remodeling in mice. *J. Clin. Invest.* 120(9), 3350–3364 (2010).

14 Nguyen Dinh Cat A, Jaisser F. Extrarenal effects of aldosterone. *Curr. Opin. Nephrol. Hypertens.* 21(2), 147–156 (2012).

15 Ji WJ, Ma YQ, Zhou X *et al*. Spironolactone attenuates bleomycin-induced pulmonary injury partially via modulating mononuclear phagocyte phenotype switching in circulating and alveolar compartments. *PLoS One* 8(11), e81090 (2013).

16 Lieber GB, Fernandez X, Mingo GG *et al*. Mineralocorticoid receptor antagonists attenuate pulmonary inflammation and bleomycin-evoked fibrosis in rodent models. *Eur. J. Pharmacol.* 718(1–3), 290–298 (2013).

• **Independent work from other group confirmed the therapeutic potential of spironolactone in acute lung injury and fibrosis.**

17 Limayem Blouza I, Charcosset C, Sfar S, Fessi H. Preparation and characterization of spironolactone-loaded nanocapsules for paediatric use. *Int. J. Pharm.* 325(1–2), 124–131 (2006).

18 Elbayoumi TA, Torchilin VP. Current trends in liposome research. *Methods Mol. Biol.* 605, 1–27 (2010).

19 Giddam AK, Zaman M, Skwarczynski M, Toth I. Liposome-based delivery system for vaccine candidates: constructing an effective formulation. *Nanomedicine (Lond.)* 7(12), 1877–1893 (2012).

20 Al-Jamal WT, Kostarelos K. Liposome-nanoparticle hybrids for multimodal diagnostic and therapeutic applications. *Nanomedicine (Lond.)* 2(1), 85–98 (2007).

21 Ahsan F, Rivas IP, Khan MA, Torres Suarez AI. Targeting to macrophages: role of physicochemical properties of particulate carriers – liposomes and microspheres – on the phagocytosis by macrophages. *J. Control. Release* 79(1–3), 29–40 (2002).

22 Roger E, Lagarce F, Garcion E, Benoit JP. Biopharmaceutical parameters to consider in order to alter the fate of nanocarriers after oral delivery. *Nanomedicine (Lond.)* 5(2), 287–306 (2010).

•• **Recent review article addressing the advantages and barriers of oral delivery of nanocarriers.**

23 Zhang K, Lv S, Li X *et al*. Preparation, characterization, and *in vivo* pharmacokinetics of nanostructured lipid carriers loaded with oleanolic acid and gentiopicrin. *Int. J. Nanomedicine* 8, 3227–3239 (2013).

24 Yuan J, Liu J, Hu Y *et al*. The immunological activity of propolis flavonoids liposome on the immune response against ND vaccine. *Int. J. Biol. Macromol.* 51(4), 400–405 (2012).

25 Otake K, Shimomura T, Goto T *et al*. Preparation of liposomes using an improved supercritical reverse phase evaporation method. *Langmuir* 22(6), 2543–2550 (2006).

26 Ji WJ, Ma YQ, Zhou X *et al*. Temporal and spatial characterization of mononuclear phagocytes in circulating, lung alveolar and interstitial compartments in a mouse model of bleomycin-induced pulmonary injury. *J. Immunol. Methods* 403(1–2), 7–16 (2014).

27 Szapiel SV, Elson NA, Fulmer JD, Hunninghake GW, Crystal RG. Bleomycin-induced interstitial pulmonary disease in the nude, athymic mouse. *Am. Rev. Respir. Dis.* 120(4), 893–899 (1979).

28 Wilson MS, Madala SK, Ramalingam TR *et al*. Bleomycin and IL-1beta-mediated pulmonary fibrosis is IL-17A dependent. *J. Exp. Med.* 207(3), 535–552 (2010).

29 Serrano-Mollar A, Closa D, Cortijo J *et al*. P-selectin upregulation in bleomycin induced lung injury in rats: effect of N-acetyl-L-cysteine. *Thorax* 57(7), 629–634 (2002).

30 Williams B, MacDonald TM, Morant S *et al*. Spironolactone versus placebo, bisoprolol, and doxazosin to determine the optimal treatment for drug-resistant hypertension (PATHWAY-2): a randomised, double-blind, crossover trial. *Lancet* 386(10008), 2059–2068 (2015).

31 Gao W, Chan JM, Farokhzad OC. pH-responsive nanoparticles for drug delivery. *Mol. Pharm.* 7(6), 1913–1920 (2010).

32 Hussell T, Bell TJ. Alveolar macrophages: plasticity in a tissue-specific context. *Nat. Rev. Immunol.* 14(2), 81–93 (2014).

• **A state-of-the-art review article on the role of alveolar macrophages in lung physiology and disease.**

33 Epelman S, Lavine KJ, Randolph GJ. Origin and functions of tissue macrophages. *Immunity* 41(1), 21–35 (2014).

34 Swirski FK, Nahrendorf M, Etzrodt M *et al*. Identification of splenic reservoir monocytes and their deployment to inflammatory sites. *Science* 325(5940), 612–616 (2009).

35 Osterholzer JJ, Olszewski MA, Murdock BJ *et al*. Implicating exudate macrophages and Ly-6C(high) monocytes in CCR2-dependent lung fibrosis following gene-targeted alveolar injury. *J. Immunol.* 190(7), 3447–3457 (2013).

36 Gibbons MA, MacKinnon AC, Ramachandran P *et al.* Ly6C^{hi} monocytes direct alternatively activated profibrotic macrophage regulation of lung fibrosis. *Am. J. Respir. Crit. Care Med.* 184(5), 569–581 (2011).

• **First paper demonstrating the Ly6C^{hi}-monocyte directed M2 polarization of alveolar macrophages in the pathogenesis of acute lung injury and fibrosis.**

37 Maus UA, Janzen S, Wall G *et al*. Resident alveolar macrophages are replaced by recruited monocytes in response to endotoxin-induced lung inflammation. *Am. J. Respir. Cell Mol. Biol.* 35(2), 227–235 (2006).

38 Janssen WJ, Barthel L, Muldrow A *et al*. Fas determines differential fates of resident and recruited macrophages during resolution of acute lung injury. *Am. J. Respir. Crit. Care Med.* 184(5), 547–560 (2011).

39 Misharin AV, Scott Budinger GR, Perlman H. The lung macrophage: a Jack of all trades. *Am. J. Respir. Crit. Care Med.* 184(5), 497–498 (2011).

40 Blasi ER, Rocha R, Rudolph AE, Blomme EA, Polly ML, Mcmahon EG. Aldosterone/salt induces renal inflammation and fibrosis in hypertensive rats. *Kidney Int.* 63(5), 1791–1800 (2003).

41 Lam EY, Funder JW, Nikolic-Paterson DJ, Fuller PJ, Young MJ. Mineralocorticoid receptor blockade but not steroid withdrawal reverses renal fibrosis in deoxycorticosterone/salt rats. *Endocrinology* 147(7), 3623–3629 (2006).

42 Sosnik A, Carcaboso AM, Glisoni RJ, Moretton MA, Chiappetta DA. New old challenges in tuberculosis: potentially effective nanotechnologies in drug delivery. *Adv. Drug Deliv. Rev.* 62(4–5), 547–559 (2010).

43 Prasad LK, O'Mary H, Cui Z. Nanomedicine delivers promising treatments for rheumatoid arthritis. *Nanomedicine (Lond.)* 10(13), 2063–2074 (2015).

44 Grobe JL, Grobe CL, Beltz TG *et al*. The brain renin–angiotensin system controls divergent efferent mechanisms to regulate fluid and energy balance. *Cell Metab.* 12(5), 431–442 (2010).

45 Engeli S, Bohnke J, Gorzelniak K *et al*. Weight loss and the renin–angiotensin–aldosterone system. *Hypertension* 45(3), 356–362 (2005).

46 Weisinger HS, Begg DP, Egan GF *et al*. Angiotensin converting enzyme inhibition from birth reduces body weight and body fat in Sprague–Dawley rats. *Physiol. Behav.* 93(4–5), 820–825 (2008).

47 Ma Z, Zhang J, Alber S *et al*. Lipid-mediated delivery of oligonucleotide to pulmonary endothelium. *Am. J. Respir. Cell Mol. Biol.* 27(2), 151–159 (2002).

48 Howard MD, Greineder CF, Hood ED, Muzykantov VR. Endothelial targeting of liposomes encapsulating SOD/catalase mimetic EUK-134 alleviates acute pulmonary inflammation. *J. Control. Release* 177, 34–41 (2014).

49 Ivanova V, Garbuzenko OB, Reuhl KR, Reimer DC, Pozharov VP, Minko T. Inhalation treatment of pulmonary fibrosis by liposomal prostaglandin E2. *Eur. J. Pharm. Biopharm.* 84(2), 335–344 (2013).

50 Yoon PO, Park JW, Lee CM *et al*. Self-assembled micelle interfering RNA for effective and safe targeting of dysregulated genes in pulmonary fibrosis. *J. Biol. Chem.* 291(12), 6433–6446 (2016).

51 Paranjpe M, Muller-Goymann CC. Nanoparticle-mediated pulmonary drug delivery: a review. *Int. J. Mol. Sci.* 15(4), 5852–5873 (2014).

52 Pozharski EV, MacDonald RC. Analysis of the structure and composition of individual lipoplex particles by flow fluorometry. *Anal. Biochem.* 341(2), 230–240 (2005).